chemistry

MDPI

Article

Fluorometric Detection of Five Nitrogen-Based Pharmaceuticals Based on Ion-Pairing Association with EY: DFT Calculations

Safanah M. Alkulaib [1], Esam M. Bakir [1,2,*] and Ahmed O. Alnajjar [1]

[1] Department of Chemistry, College of Science, King Faisal University, Al-Ahsa 31982, Saudi Arabia; salkulaib@kfu.edu.sa (S.M.A.); anajjar@kfu.edu.sa (A.O.A.)
[2] Department of Chemistry, Faculty of Science, Ain shams University, Cairo 11566, Egypt
* Correspondence: ebakir@kfu.edu.sa

Abstract: Fluorometric method for detecting of five nitrogen-based drugs concentration based on inhibition of emission Eosin Y (EY). The selection of N-drugs comprised indapamide (INDP), clomipramine hydrochloride (CMI), promethazine hydrochloride (PMH), lisinopril (LSP), and trifluoperazine hydrochloride (TFPH). The Stern–Volmer style was plotted between relative emissions of EY vs. N-drugs concentration. The standard curves were linear over the concentration range of 5–50 μg mL^{-1} with $R^2 > 0.9$, and the LOD for INDP, CMI, PMH, LSP, and TFPH were 2.07, 1.36, 3.02, 3.52, and 2.09 μmol·L^{-1}, respectively. The binding constant K_{app} for LSP was greater than other N-drugs. Furthermore, the suggested method was hence applied for the routine detection of the concentration of N-drugs in bulk and tablet or syrup dosage forms. FTIR analysis and the electron-mapping density provided the chemical affinity of N-drugs towards EY.

Keywords: N-drugs; Eosin Y fluorescent; ion-pairing; chemical affinity

1. Introduction

Nitrogen group-based drugs are used as therapeutics for a wide range of diseases. Indapamide and Lisinopril were used as treatment for hypertension and heart failure, respectively [1,2]. The basis of drug configuration depends on stereochemistry location of nitrogen atoms such as primary-, secondary-, or tertiary-type (Figure 1) Indapamide (INDP), 4-chloro-N-(2-methyl-1-indolinyl)-3-sulfamoylbenzamide [3]. Lisinopril (LSP) is N2–[(1S)-1-carboxy-3-phenylpropyl]-L-lysyl]-L-proline dehydrate [4]. Promethazine prevented the nausea and vomiting related to certain conditions. The empirical formula for promethazine hydrochloride (PMH) is N,N-dimethyl-1-(10H-phenothiazin-10-yl) propan-2-amine hydrochloride (C17H20N2S.HCl) [5]. Trifluoperazine HCl is 10-[3-(4-methyl-1-piperazinyl)propyl]-2-(trifluoromethyl)-10H-phenothiazine dihydrochloride [6] and helps reduce hallucinations (hearing/seeing things that are not there) [3]. Clomipramine is also known as 3-(3-chloro-10,11-dihydro-5H-dibenzo[b,f]azepin-5-yl)-N,N-dimethylpropan-1-amine [7], which is commonly used to treat obsessive–compulsive disorder (OCD) [8].

The HPLC method [9–11], electrophoretic technique [12], chemiluminescence [13], electroanalytical approaches [14], and colorimetric assay [15,16] succeed in detecting the drugs concentration in raw form and formulation. However, HPLC methods should study the experiment conditions such as high-grade solvents, sampling, and type of detectors. Furthermore, the spectrophotometric method is less sensitive than the spectrofluorometric method. The advantages of the fluorometric method were obtained in the form of simplicity, selectivity, and high sensitivity. Eosin Y as fluorescent dye and lead ions were used in the determination of indapamide concentration. The fluorometric method was studied for the decay of fluorescence emission of EY based on the formation of ternary complexes [17].

check for updates

Citation: Alkulaib, S.M.; Bakir, E.M.; Alnajjar, A.O. Fluorometric Detection of Five Nitrogen-Based Pharmaceuticals Based on Ion-Pairing Association with EY: DFT Calculations. *Chemistry* **2024**, *6*, 981–992. https://doi.org/10.3390/chemistry6050057

Received: 21 June 2024
Revised: 29 August 2024
Accepted: 30 August 2024
Published: 10 September 2024

Copyright: © 2024 by the authors. Licensee MDPI, Basel, Switzerland. This article is an open access article distributed under the terms and conditions of the Creative Commons Attribution (CC BY) license (https://creativecommons.org/licenses/by/4.0/).

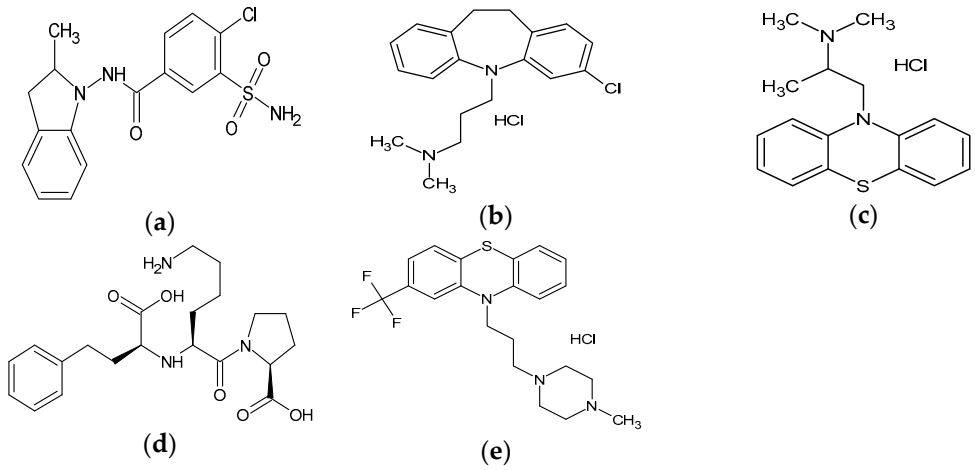

Figure 1. The chemical structure of (**a**) INDP, (**b**) CMI, (**c**) PMH, (**d**) LSP, and (**e**) TFPH.

The charge transfer process between EY and drug molecule was studied in the determination of the promethazine through the formation of binary complexes. Furthermore, the charge transfer process was approved between promethazine as an electron donor and a strong electron acceptor EY [18].

Herein, we supplied a simple and sensitive spectrofluorometric method for detection of the concentration of drugs having nitrogen groups in raw and pharmaceutical formula such as indapamide, lisinopril, promethazine, trifluoperazine, and clomipramine. The novelty of this study is that it is the first to detect the concentration five drugs which contain primary, secondary, and tertiary nitrogen groups. The inhibition of EY emission was selective and sensitive for each drug, which are represented by k_q and Kapp values.

The designed system was used to detect the drug concentrations based on the "on-off" fluorescence emission of Eosin Y with complex formation. The fluorescence quenching reaction was directly matched to the drug concentration. The fluorometric method was a very simple and sensitive route for drug detection. The fluorometric method had properties such as an inexpensive EY reagent and easily applied; the equipment used is widely available in most quality control laboratories. Next, we describe the chemical affinity of EY to form ion-pair complexes with drugs that were studied by density functional theory (DFT) based on electron-mapping density.

2. Experimental Section

2.1. Materials and Reagents

Eosin Y, Indapamide (INDP) (99%), Clomipramine hydrochloride (CMI) (99%), Promethazine hydrochloride (PMH) (99%), Lisinopril (LSP) (98%), Trifluoperazine hydrochloride (TFPH) (99%) were received from Sigma Aldrich, Al Khobar, Saudi Arabia. HPLC high-grade solvents were used. The designed system of the formation of the drug–EY complex was performed in acetate buffer at pH 3.50. In the fluorometric assay, the materials are used without further purification, and freshly prepared solutions are prepared daily. The Normalix SR 1.50 mg/g tablet of indapamide (Jazeera pharmaceutical industries, Riyadh, Saudi Arabia), Anafranil 10 mg/tablet of clomipramine HCl (Novartis, London, UK), PROMETIN syrup 5.0/5 mL of promethazine-HCl (Kuwait Saudi pharmaceutical industries, Kuwait, Kuwait), Zestril 5 mg/g of lisinopril (Astra Zeneca, London, UK), and Stellasil 5 mg/g tablet of trifluoperazine HCl (Kahira Pharmaceuticals & chemical Industries company, Cairo, Egypt) were received from the Saudi local market.

2.1.1. Practical Steps of the Designed Method

The ethanolic stock solution of 1.0 mM EY was used. The stock solutions of 1.0 mmol·L^{-1} drugs were prepared in the appointed solvent. The solutions were kept in a refrigerator (4 °C). A 1.0 mL quantity of (10–100 µmol L^{-1}) N-drugs was added to

1.0 mL (10 µmol L^{-1}) Eosin Y with a completed 10 mL measuring flask by acetate buffer and adjusted at pH 3.50. The solutions were left for 8 min to complete the formation of an ion-pairing complex EY/drug. The blank reagent was run in parallel with the same criteria except for the drug solution. The fluorescence-off effect of N-drugs on EY emission intensity was measured using the fluorometric technique. The fluorescence intensity values of the EY–drug solutions were plotted vs. drug concentration (µmmol L^{-1}) at λ_{em} 550 nm. The regression model (y = ax + b) was used to calculate the drug concentrations. The Shimadzu spectrophotometer model and Ocean-Optics FL4000 (Ocean Optics, Orlando, USA) spectrofluorometer model were used to measure the UV–visible and emission spectra of EY and their complexes. An alpha bruker FTIR spectrometer (Bruker devices, Santa Barbara, CA, USA) OPUS was used for investigating the vibrational frequency of EY groups in the ion-pairing system.

2.1.2. Commercial Pharmaceutical Formulation Analysis

Five tablets from the sold drugs were ground in a mortar. The amount of powder was weighed and dissolved in methanol. After 10 min of sonication, the mixture was centrifuged at 1800× rpm for 5 min, and the supernatant was filtered through Whatman filter paper. The precipitate was washed several times with the solvent. The filtrate was made up to 100 mL with methanol. The procedure was repeated for different tablets, and measurements were made in duplicate. For the syrup sample, 1.0 mL of syrup was added in a 10 mL volumetric flask, then filled with 80% volume with methanol. The solution was sonicated for 15 min to ensure homogeneity. Leave the solution at room temperature, and then complete the flask to the mark by methanol. According to this procedure, the final solution should have a drug concentration of 0.1 mg/mL.

3. Results and Discussion

3.1. The Design System Spectra

The absorbance and emission spectra of EY were measured in the absence and presence of N-drug (see Figure 2a,b). The absorbance and fluorescence spectra of EY showed a strong visible band at 530 nm corresponding to the π-*π transition with high emission appearing at 550 nm [19,20]. The quenching of EY emission was observed by adding N-drug concentrations to the acetate buffer at pH = 3.5. The changes in the absorption and emission spectra of EY were obtained after adding N-drugs due to the formation of the ion-pairing system.

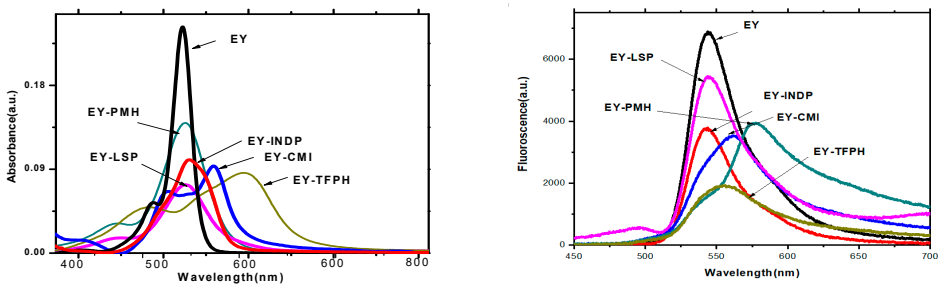

(**a**) (**b**)

Figure 2. The absorbance (**a**) and emission spectra (**b**) of 10 µmol·L^{-1} of EY before and after adding 50 µmol·L^{-1} of N-drugs as follows: INDP, CMI, PMH, LSP, and TFPH in acetate buffer (pH = 3.5).

3.2. Stern–Volmer and Benesi–Hildebrand Formula

The Stern–Volmer theory was applied to describe the quenching process between EY and N-drugs. The Stern–Volmer style was plotted between the relative emission of EY

in the absence and presence of N-drug as quencher [Q], as seen in Equation (1) [21] (see Figure 2).

$$\frac{f_0}{f}(\Delta f) = 1 + k_{sv}[Q] = 1 + k_q\tau_0[Q] \quad (1)$$

The Stern–Volmer constant (k_{sv}) is the slope, and the quenching rate constant k_q ($k_{sv} = k_q\tau_0$) is equal to the multiplication of k_{sv} and lifetime (τ_0), where τ_0 (2.66 ns) is the lifetime of Eosin Y [22]. Stern–Volmer plots and k_q values were used to explain the quenching process mechanism between drug–EY collisions. The Stern–Volmer plots were obtained with linearity and high k_q values (Table 1 and Figure 3). The quenching process of EY emission was carried out through the static collision mechanism [23,24].

Table 1. Stern–Volmer and Benesi–Hildebrand relations for EY–drugs ion-pairing complexes.

N-Drugs	Stern–Volmer Parameters			Benesi–Hildebrand	
	$k_{sv} \times 10^4$ (L·mol^{-1})	$k_q \times 10^{12}$ (L·mol^{-1}·s^{-1})	R^2	$K_{app} \times 10^4$	R^2
INDP	1.60	1.90	0.97	1.02	0.94
CMI	2.60	3.20	0.98	0.83	0.97
PMH	3.90	4.70	0.97	1.59	0.96
LSP	6.90	8.30	0.98	1.76	0.96
TFPH	4.35	4.88	0.98	1.49	0.96

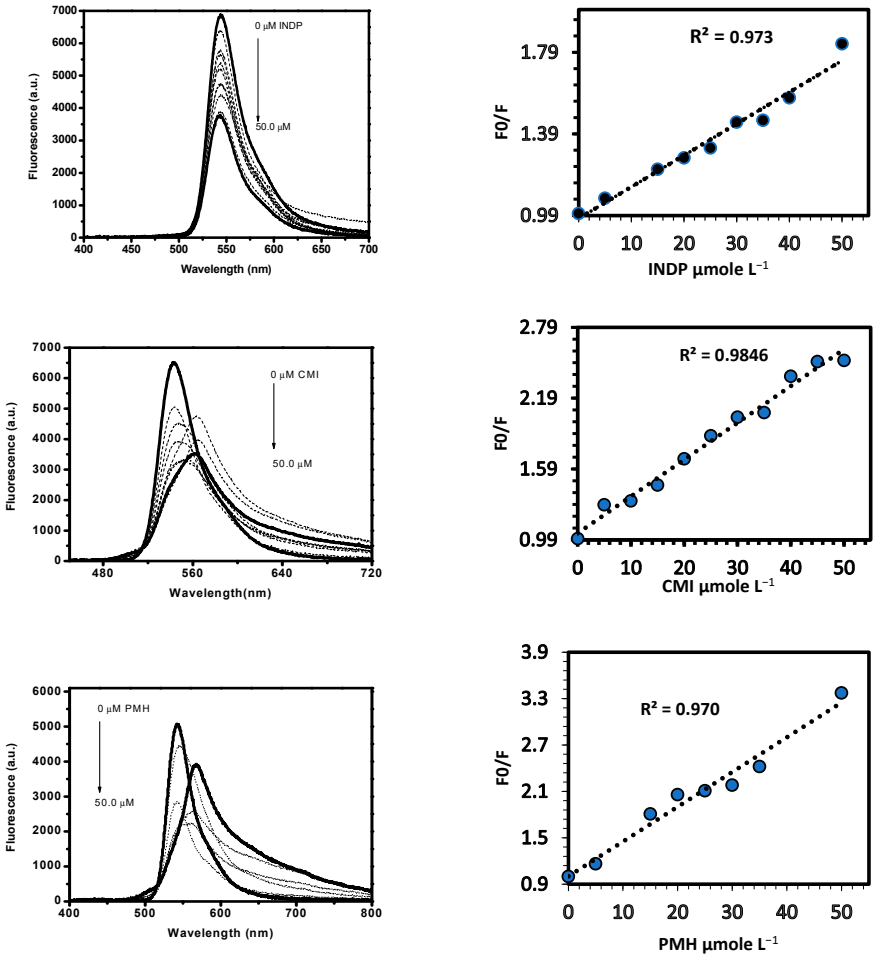

Figure 3. *Cont.*

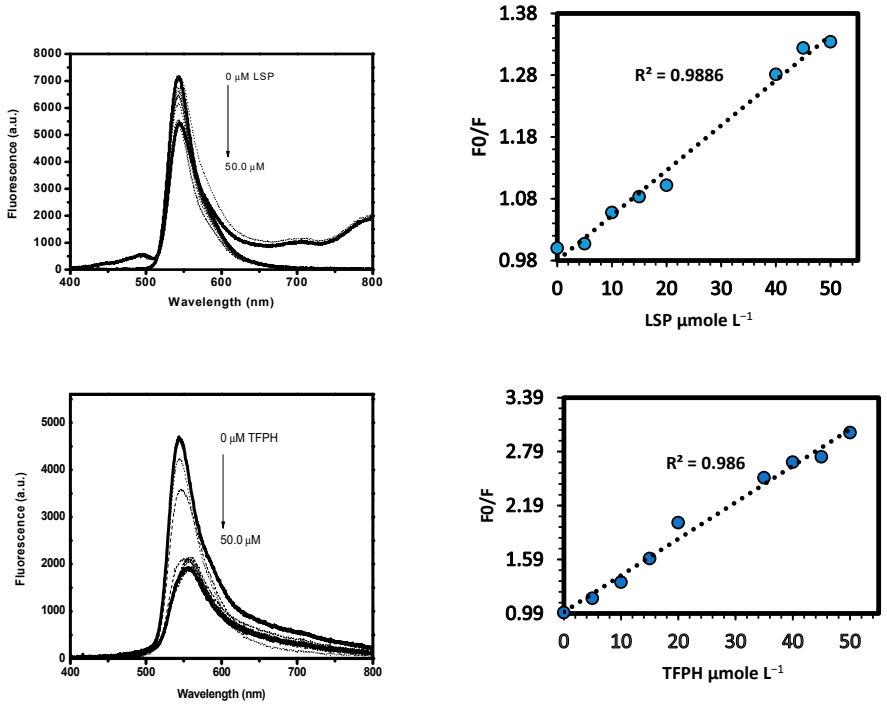

(**a**) (**b**)

Figure 3. The emission spectra (**a**) and (**b**) calibration curves of 10 µmole L^{-1} EY with addition of 5.0–50 µmole L^{-1} N-drugs in the acetate buffer (pH = 3.50).

The binding association constants (K_{app}) were calculated from the absorbance spectra of EY and N-drugs by applying the Benesi–Hildebrand relationship, (Equation (2)) [25]

$$log\frac{(A - A_0)}{(A_f - A_0)} = logK_{app} + log[D] \quad (2)$$

where A_0, A, and A_f are the absorption values, in the absence of N-drug, at the intermediate and at the saturation of the interaction of EY with drug respectively, and $[D]$ is the N-drugs concentration. The high K_{app} values were obtained due to the strong formation of the ion-pairing EY/N-drugs system (Table 1).

3.3. The Molar Ratio N-Drugs with EY

The molar ratio method was used to detect the mole ratio of ion-pairing EY/N-drugs system [26]. The ion-pairing system of N-drugs/EY was formed by electrostatic attraction of the acidic carboxylic acid group or -OH group of EY and the alkaline moiety (amino group) of the N-drug [27]. The molar ratio was 2:1 for the EY/N-drugs ion-pairing system.

4. Methods Validation

The fluorometric method was validated according to ICH guidelines [28]. The validation parameters such as linearity, dynamic range, detection (LOD), and quantitation (LOQ) limits, precision, and accuracy were calculated from the regression model analysis.

4.1. Linearity and Range

The linearity of the designed fluorometric method was obtained by using a series of standard solutions of the drug. The calibration curves were plotted between relative emission of EY vs. N-drug concentration. The linearity was 5.0–50.0 µmol L^{-1} for N-drugs with ($R^2 > 0.9$).

The detection (LOD) and quantification (LOQ) limits were calculated from the calibration curves of the regression model of the fluorometric method according to the following Equation (3).

$$LOD = 3.3\,\sigma/S, LOQ = 10.0\,\sigma/S \quad (3)$$

where S is the slope of the calibration curve, and σ is the standard deviation of the YX straight line of regression analysis [29]. The LOD and LOQ values were 2.07,1.36, 3.02, 3.52, and 4.20 µM for, INDP, CMI, PMH, LSP, and TFPH, respectively (see Table 2).

Table 2. The detection and quantification limits of the fluorometric method.

N-Drugs	LOD (µM)	LOQ (µM)
INDP	2.07	6.30
CMI	1.36	4.11
PMH	3.02	9.20
LSP	3.32	10.07
TFPH	4.20	12.67

4.2. Accuracy and Precision

The accuracy of the fluorometric method was used at three concentration levels (8.0, 15.0, and 30.0 µM). The fluorometric method obtained a good recovery, as seen in Table 3. Furthermore, the precision was examined with inter-day and intra-day precision levels. The % RSD values of the fluorometric method were found at the acceptance value of 2.0%.

Table 3. Accuracy and precision levels of the fluorometric method at three concentration levels of the studied drug.

N-drugs	Concentration Levels (µM)	Recovery% ±SD	Precision Level, RSD%	
			Inter-Day	Intra-Day
INDP	8.0, 15.0, 30.0	100.3 ± 0.78	0.73	1.68
CMI	8.0, 15.0, 30.0	100.36 ± 0.83	0.74	1.73
PMH	8.0, 15.0, 30.0	100.84 ± 1.82	1.66	1.71
LSP	8.0, 15.0, 30.0	100.22 ± 0.65	0.57	1.32
TFPH	8.0, 15.0, 30.0	100.16 ± 0.49	0.42	1.63

4.3. Pharmaceutical Formula

The fluorometric method was used to find the concentration of drugs in its pharmaceutical formula. The paired t-test was used to examine the quality of the % recovery of the fluorometric method (Table 4). At limit of confidence level 95%, the obtained paired *t*-values were less than the *t*-values tabulated values, so there are no systematic errors in the determination of the precision and accuracy of the fluorometric method. Furthermore, the high recovery values with no interference from the other components of formula packs were obtained, so the fluorometric method is suitable for detecting the drug-containing dosage forms and assays in QC laboratories.

Table 4. Analysis of the studied drug in its pharmaceutical dosage form using the designed method.

Pharmaceuticals Formula	The Proposed Method, n = 5	
	% Recovery ± SD	Paired *t*-Value and Tabulated *t* *
Normalix SR (1.50 mg) INDP	100.16 ± 1.01	0.70
Anafranil (10 mg) CMI	99.93 ± 0.65	0.61

Table 4. *Cont.*

Pharmaceuticals Formula	The Proposed Method, n = 5	
	% Recovery ± SD	Paired *t*-Value and Tabulated *t* *
PROMETIN syrup (5.0/5 mL) PMH	99.27 ± 2.22	1.49
Zestril (5 mg/g) LSP	99.82 ± 1.63	0.48
Stellasil (5 mg/g) TFPH	99.42 ± 2.38	1.40

* Tabulated *t*-value was 2.771, degree of freedom n − 1 = 5.

4.4. The Chemical Affinity of N-Drugs towards EY

The ion-pairing process played an important role in detecting the quantity of drug and the affinity of drug molecule towards Eosin Y to form the ion-pairing system. Firstly, the Eosin Y molecule takes various forms, including neutral, mono-anionic, and di-anionic species, depending on the pH of the medium. At pH = 3.50, mainly neutral and mono-anionic forms are found, while at pH > 7, the di-anions form was showed. The absorbance and fluorescence spectra of EY were dependent on the pH of the EY solution [30,31]. The quantum yield Φ of fluorescence intensity of EY was increased by increasing the pH due to the existence of di-anions forms. The -OH hydroxyl group in EY was slightly more ionized than the -COOH carboxyl group, where -OH besides the bromine atoms acts as a strong electron-withdrawing group which accelerated the ionization of -OH over the -COOH group. Furthermore, the amino group of the drug molecule was easily ionized in acidic media, with the formation of cationic form at the nitrogen center. The ion-pair drug–EY complex was formed between the EY-negative (-O) center and the drug-positive (N^+) center [32,33]. The binding affinities and charge transfer processes in EY–drug ion pairing play a role in the detection of the drug concentration and explain the strength of the drug–EY complex. FTIR spectra were applied to confirm the location of binding between EY and drug molecule. The FTIR spectrum showed EY bands of -OH and -COOH groups, and a changing feature was found in the IR spectrum that confirmed the formation of the ion-pairing complex. It was concluded that the -OH groups in the EY molecule were changed, confirming the bonding with the drug molecule [33] (Figure 4).

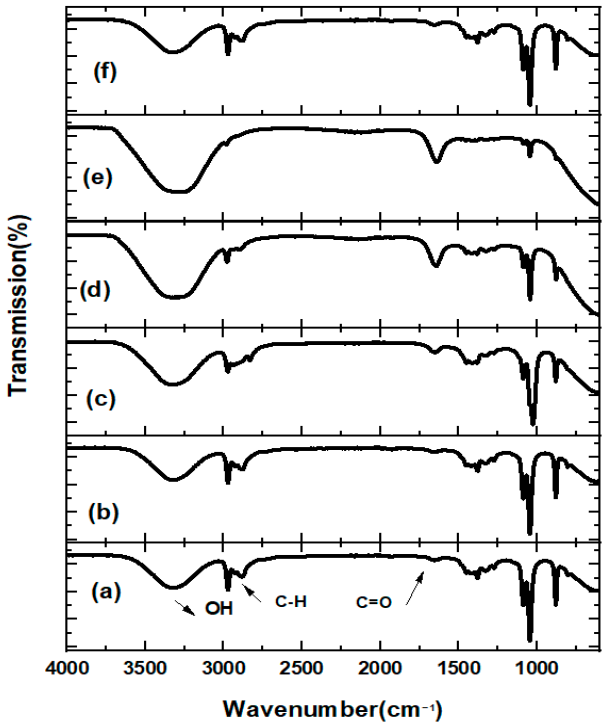

Figure 4. FTIR spectra of EY (**a**) and their ion-pairing systems of INDP (**b**), CMI (**c**), PMH (**d**), LSP (**e**), and TFPH (**f**).

4.5. Computational Calculations

Theoretical calculations based on density functional theory (DFT) were carried out using the Gaussian G09W program. All compounds were optimized according to Beckers three-parameter exchange functional with basis set B3LYP/6-31G*[34,35]. The Electron affinity (EA), Ionization energy (IE), hardness and softness, and the HOMO, LUMO are calculated. The chemical affinity of EY to form ion-pairing complexes with drugs was examined using DFT calculations [36]. The energy gap (Eg), E_{HOMO} and E_{LUMO}, chemical hardness (η), Softness (S), the electronic chemical potential (μ), and electrophilicity (ω) are calculated via Equations (3)–(7); these parameters were added to confirm the global reactivity of the EY molecule [37,38]:

$$\text{Eg} = E_{HOMO} - E_{LUMO} \tag{4}$$

$$\eta = (E_{LUMO} - E_{HOMO})/2 \tag{5}$$

$$s = \frac{1}{\eta} \tag{6}$$

$$\mu = \frac{1}{2}(E_{LUMO+}E_{HOMO}) \tag{7}$$

$$\omega = \frac{\mu^2}{2\eta} \tag{8}$$

Electrochemical potential (μ) plays an important role in proving the ability of electron transfer between EY and drug [37]. In general, the harder the molecule, the less reactive it is to reactions [38]. Here, the electron potential (μ) of the EY di-anion is larger than that of the mono-COO and -OH species, showing that the EY di-anion possesses high electron exchange with drug molecules. Although, the chemical potential and electrophilicity values of the drugs suggest that INDP is highly reactive given that it is a potent donor molecule. The EY di-anion species have the lowest chemical hardness (η) and are accessible through electron exchange with the indicated drug compound (host–guest) interaction (Table 5).

Table 5. Represented HOMO and LUMO energies, hardness (η), softness (S), chemical potential (μ) and electrophilicity (ω) of EY forms (mono- anions and di-anion) of EY and drug molecules.

Molecules	E(eV) HOMO	E(eV) LUMO	Eg (eV)	η	S	μ	ω
EY/di-anions	1.19	3.68	−2.49	1.24	0.81	2.44	2.391
EY/mono (COO^-)	−1.46	1.05	−2.52	1.26	0.79	−0.21	0.008
EY/mono (-OH)	−2.06	0.44	−2.50	1.25	0.80	−0.81	0.262
INDP	−5.4	−1.9	−3.4	1.75	0.57	−3.65	3.776
CMI	−5.3	−0.2	−5.1	2.55	0.39	−2.75	1.495
PMH	−5.1	−0.2	−4.9	2.45	0.41	−2.65	1.433
LSP	−5.6	−0.4	−5.2	2.60	0.38	−3.00	1.730
TFPH	−4.7	−0.9	−3.8	1.90	0.53	−2.80	2.063

A molecular electrostatic potential map enables the exploration of molecular sites susceptible to electrophilic or nucleophilic attacks. Probing changes in electrostatic potential are an indication of the local reactivity within a molecule. Computationally, we achieve this by directing a positive charge towards the molecule. The molecular regions with high electron density should interact easily with the positive charge; therefore, a site with low electrostatic potential develops at the interaction area. In contrast, a low electron density site should give rise to a high electrostatic potential upon rippling interaction with the positive charge. We then label the low electrostatic potential sites (electron-rich) with a red color, and the regions with high electrostatic potential (electron-poor) with a

blue color. We then label the areas with moderate interaction using colors between red and blue, which represent areas with a moderate electron population. The MEP maps for the EY species and drug molecules were derived using B3LYP/3-12G calculations and the GaussView 6 graphical interface, as shown in Figure 5. The map shows that $EY-(O^-)$ has wider electron-rich regions (indicated by the red color) than $EY-(COO^-)$ and more intense than EY, which give rise to enhanced electron donation in the order $EY-(O^-) > EY-(COO^-) > EY$. The more electron-rich sites, the more chances for the reallocation of the HOMO of the donor to the LUMO of the acceptor. On the other hand, the maps of the drug molecules show remarkable electrophilic molecular sites ranging from extreme high electrostatic potential sites (blue-colored areas) to moderate electrostatic potential sites (green- and yellow-colored areas), which make them good candidates for the interaction with the $EY-(O^-)$, $EY-(COO^-)$ and EY molecules. It is worth mentioning that LUMO(s) of CMI and PHM molecules have more locations to accept the charge than the LUMO(s) of INDP, LSP, and TEPH molecules (Figure 5).

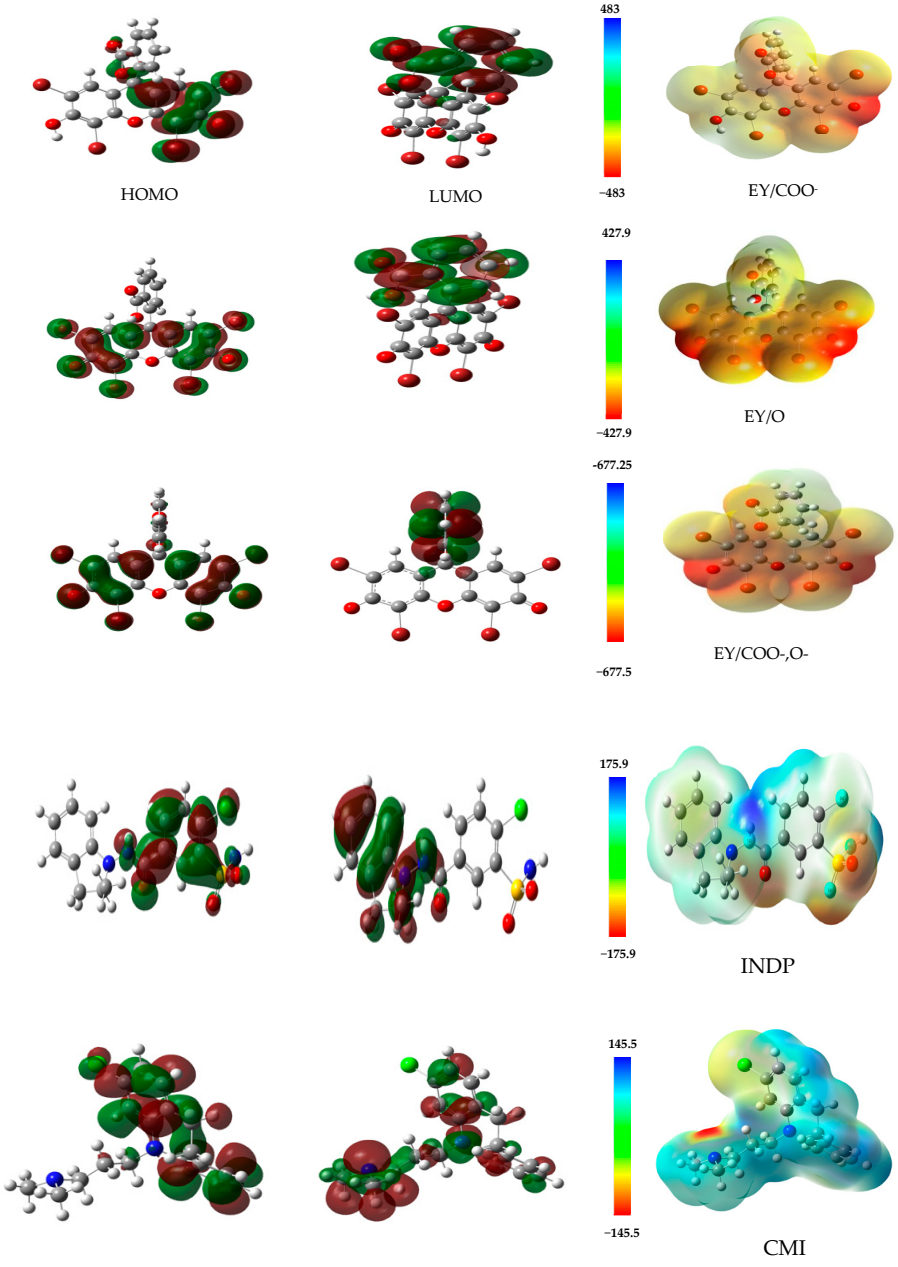

Figure 5. *Cont.*

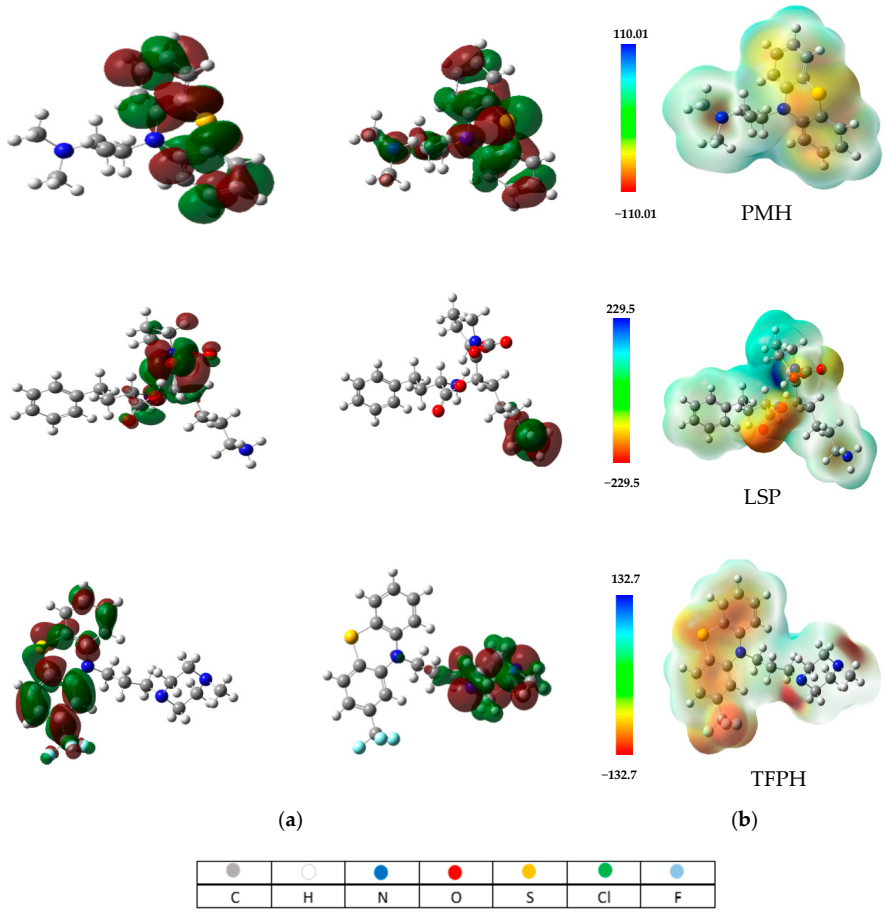

Figure 5. (**a**) Distribution of HOMO and LUMO orbitals of the cited drugs and mono- and di-anions species of EY and (**b**) Electron density map (kJ/mol).

The electrostatic potential (MEP) is a highly effective tool to predict the reactive sites of the molecule with the target molecule [39]. The electrophilic and nucleophilic regions of the EY species and drug molecules are shown in Figure 5. The large electronegative region (red color iso-surface) found in a nucleophilicity location at -OH was greater than the -COOH group. The primary NH_2- was in a greater electrophilicity location than the secondary and tertiary N-groups in the N-drugs. So, the electrophilic attack, and a large positive region (blue color iso-surface), are seen on the PC's cation, which is prone to nucleophilic attack.

5. Conclusions

The study utilized a fluorometric approach to measure the concentration of five different drugs containing nitrogen, and it focused on the inhibition of Eosin Y (EY) emission. The N-drugs that were chosen include indapamide (INDP), clomipramine hydrochloride (CMI), promethazine hydrochloride (PMH), lisinopril (LSP), and trifluoperazine hydrochloride (TFPH). The Stern–Volmer method was employed to graph the relative emissions of EY in relation to the concentration of N-drugs. The standard curves exhibited a linear relationship within the concentration range of 5–50 μg mL^{-1}, with a coefficient of determination (R^2) greater than 0.9. The suppression of EY emission was specific and responsive to each drug, as indicated by the k_q and K_{app} values. The INDP, CMI, PMH, LSP, and TEPH concentrations in pharmaceutical formulations were determined using a straightforward, affordable, highly sensitive, and quick spectrofluorometric approach. The chemical reactivity of EY and N-drugs was analyzed using density functional theory (DFT). FTIR and the ESP (electronic surface potential mapping) analysis were provided and confirmed the formation of N-drugs/EY ion-pairing. The investigation of LUMO and HOMO and MEP maps agreed well with the experimental findings.

Author Contributions: Conceptualization, S.M.A., E.M.B. and A.O.A.; methodology, S.M.A. and E.M.B.; software, E.M.B.; validation S.M.A., E.M.B. and A.O.A.; formal analysis, E.M.B.; investigation, S.M.A., E.M.B. and A.O.A.; resources, S.M.A., E.M.B. and A.O.A.; data curation, E.M.B.; writing—original draft preparation, S.M.A., E.M.B. and A.O.A.; writing—review and editing, E.M.B.; visualization, S.M.A., E.M.B. and A.O.A.; supervision, E.M.B. and A.O.A.; project administration, E.M.B. and A.O.A.; funding acquisition, S.M.A., E.M.B. and A.O.A. All authors have read and agreed to the published version of the manuscript.

Funding: The authors extend their appreciation to the deanship of scientific research King Faisal University in Saudi Arabia, for funding this research work (KFU241633).

Data Availability Statement: All data generated or analyzed during this study are included in this published article.

Acknowledgments: The authors express their deepest gratitude for King Faisal University, P.O box 400, Al-Ahsa, Postcode: 31982, Kingdom of Saudi Arabia.

Conflicts of Interest: The authors declare no conflicts of interest.

References

1. Thomas, J.R. A review of 10 years of experience with indapamide as an antihypertensive agent. *Hypertension* **1985**, *7*, 152. [CrossRef] [PubMed]
2. Goa, K.L.; Haria, M.; Wilde, M.I. Lisinopril. A review of its pharmacology and use in the management of the complications of diabetes mellitus. *Drugs* **1997**, *53*, 1081–1105. [CrossRef] [PubMed]
3. Vardanyan, R.S.; Hruby, V.J. 16-Antihistamine Drugs. In *Synthesis of Essential Drugs*; Vardanyan, R.S., Hruby, V.J., Eds.; Elsevier: Amsterdam, The Netherlands, 2006; pp. 219–235. [CrossRef]
4. Wu, M.; Douglas, A.; Ondeyka, D.; Payne, L.; Ikeler, T.; Joshua, H.; Patchett, A. Synthesis of N2-[(S)-1-carboxy-3-phenylpropyl]-L-lysyl-L-proline (lisinopril). *J. Pharm. Sci.* **1985**, *74*, 352–354. [CrossRef] [PubMed]
5. Shearer, C.M.; Miller, S.M. Promethazine Hydrochloride. In *Analytical Profiles of Drug Substances*; Florey, K., Ed.; Academic Press: Cambridge, MA, USA, 1976; pp. 429–465. [CrossRef]
6. Post, A.; Warren, R.J.; Zarembo, J.E. Trifluoperazine Hydrochloride. In *Analytical Profiles of Drug Substances*; Florey, K., Ed.; Academic Press: Cambridge, MA, USA, 1981; pp. 543–581. [CrossRef]
7. Chaudhuri, N.K.; Sung, M.S.; Markus, B. Synthesis of clomipramine-d8. *J. Label. Compd. Radiopharm.* **1981**, *18*, 1817–1825. [CrossRef]
8. Van Scheyen, J.D.; Van Kammen, D.P. Clomipramine-induced mania in unipolar depression. *Arch. Gen. Psychiatry* **1979**, *36*, 560–565. [CrossRef]
9. Bahgat, E.A.; Saleh, H.; Reda, A.; Fawzy, M.G. Development and validation of eco-friendly micellar organic solvent-free HPLC method for the simultaneous determination of some antihypertensive combinations. *Microchem. J.* **2022**, *181*, 107740. [CrossRef]
10. Rodina, T.; Melnikov, E.; Aksenov, A.; Belkov, S.; Sokolov, A.; Prokof'ev, A.; Ramenskaya, G. Simultaneous Determination of Dabigatran, Rivaroxaban, Apixaban, and Warfarin in Human Blood Serum by HPLC-MS/MS for Therapeutic Drug Monitoring. *Pharm. Chem. J.* **2022**, *56*, 289–293. [CrossRef]
11. Bezawada, V.; Mogili, P.; Dodda, S.; Gajula, R.; Ponnada, S. Bioanalysis of Trifluoperazine in human plasma by LC-MS/MS: Application to disposition kinetics. *Biomed. Chromatogr.* **2022**, *36*, e5499. [CrossRef]
12. Ermolenko, Y.; Nazarova, N.; Belov, A.; Kalistratova, A.; Ulyanova, Y.; Osipova, N.; Gelperina, S. Potential of the capillary electrophoresis method for PLGA analysis in nano-sized drug formulations. *J. Drug Deliv. Sci. Technol.* **2022**, *70*, 103220. [CrossRef]
13. Budziñski, M.L.; Sokn, C.; Gobbini, R.; Ugo, B.; Antunica-Noguerol, M.; Senin, S.; Bajaj, T.; Gassen, N.C.; Rein, T.; Schmidt, M.V.; et al. Tricyclic antidepressants target FKBP51 SUMOylation to restore glucocorticoid receptor activity. *Mol. Psychiatry* **2022**, *27*, 2533–2545. [CrossRef]
14. Al–Farhan, B.S.; Gahlan, A.A.; Haredy, A.M.; Fraghly, O.A. Cathodic Stripping Voltammetric Determination of Lisinopril in Dosage Forms and Biological Fluids. *Egypt. J. Chem.* **2022**, *65*, 421–428. [CrossRef]
15. Raja, D.A.; Shah, M.R.; Malik, M.I. Polyethyleneimine stabilized silver nanoparticles as an efficient and selective colorimetric assay for promethazine. *Anal. Chim. Acta* **2022**, *1223*, 340216. [CrossRef] [PubMed]
16. Miyoshi, H.; Otomo, M.; Takahashi, K. Clomipramine inhibits dynamin L-α-phosphatidyl-L-serine stimulated GTPase activity. *J. Biochem.* **2022**, *174*, 267–272. [CrossRef] [PubMed]
17. Omar, M.A. Spectrophotometric and Spectrofluorimetric Determination of Certain Diuretics Through Ternary Complex Formation with Eosin and Lead (II). *J. Fluoresc.* **2010**, *20*, 275–281. [CrossRef]
18. Molnår, J.; Földeák, S.; Nakamura, M.J.; Gaizer, F.; Gutmann, F. The influence of charge transfer complex formation on the antibacterial activity of some tricyclic drugs. *Xenobiotica* **1991**, *21*, 309–316. [CrossRef]
19. Kathiravan, A.; Anbazhagan, V.; Jhonsi, M.A.; Renganathan, R. A Study on the fluorescence quenching of eosin by certain organic dyes. *Z. Phys. Chem.* **2008**, *222*, 1013–1021. [CrossRef]

20. Ganguly, B.; Nath, R.K.; Hussain, S.A.; Panda, A.K. Photophysical studies of xanthene dye in alkanols and in presence of inorganic ions. *Indian J. Phys.* **2010**, *84*, 653–658. [CrossRef]
21. Boaz, H.; Rollefson, G.K. The Quenching of Fluorescence. Deviations from the Stern-Volmer Law. *J. Am. Chem. Soc.* **1950**, *72*, 3435–3443. [CrossRef]
22. Fleming, G.R.; Knight, A.W.E.; Morris, J.M.; Morrison, R.J.S.; Robinson, G.W. Picosecond fluorescence studies of xanthene dyes. *J. Am. Chem. Soc.* **1977**, *99*, 4306–4311. [CrossRef]
23. Lakowicz, J. *Principles of Fluorescence Spectroscopy*, 3rd ed.; Plenum Press: New York, NY, USA, 1986. [CrossRef]
24. Arık, M.; Çelebi, N.; Onganer, Y. Fluorescence quenching of fluorescein with molecular oxygen in solution. *J. Photochem. Photobiol. A Chem.* **2005**, *170*, 105–111. [CrossRef]
25. Benesi, H.A.; Hildebrand, J.H. A spectrophotometric investigation of the interaction of iodine with aromatic hydrocarbons. *J. Am. Chem. Soc.* **1949**, *71*, 2703–2707. [CrossRef]
26. Mabrouk, M.; Hammad, S.F.; Abdelaziz, M.A.; Mansour, F.R. Ligand exchange method for determination of mole ratios of relatively weak metal complexes: A comparative study. *Chem. Cent. J.* **2018**, *12*, 143. [CrossRef]
27. Omar, M.A.; Ahmed, A.B.; Abdelwahab, N.S.; Abdelrahman, M.M.; Derayea, S.M. Spectrofluorimetric approach for determination of citicoline in the presence of co-formulated piracetam through fluorescence quenching of eosin Y. *Spectrochim. Acta Part A Mol. Biomol. Spectrosc.* **2020**, *236*, 118337. [CrossRef]
28. Walfish, S. Analytical methods: A statistical perspective on the ICH Q2A and Q2B guidelines for validation of analytical methods. *BioPharm Int.* **2006**, *19*, 40–45.
29. Guideline, I.H.T. Validation of Analytical Procedures: Text and Methodology Q2 (R1). In Proceedings of the International Conference on Harmonization, Geneva, Switzerland, 2 June 2005.
30. Slyusareva, E.; Gerasimova, M. pH-dependence of the absorption and fluorescent properties of fluorone dyes in aqueous solutions. *Russ. Phys. J.* **2014**, *56*, 1370–1377. [CrossRef]
31. Chakraborty, M.; Panda, A.K. Spectral behaviour of eosin Y in different solvents and aqueous surfactant media. *Spectrochim. Acta Part A Mol. Biomol. Spectrosc.* **2011**, *81*, 458–465. [CrossRef] [PubMed]
32. Salim, M.M.; Marie, A.A.; Kamal, A.H.; Hammad, S.F.; Elkhoudary, M.M. Using of eosin Y as a facile fluorescence probe in alogliptin estimation: Application to tablet dosage forms and content uniformity testing. *Spectrochim. Acta Part A Mol. Biomol. Spectrosc.* **2023**, *285*, 121919. [CrossRef]
33. Hamad, A.A.; Ali, R.; Derayea, S.M. A simple single jar "on–off fluorescence" designed system for the determination of mitoxantrone using an eosin Y dye in raw powder, vial, and human biofluids. *RSC Adv.* **2022**, *12*, 7413–7421. [CrossRef]
34. Becke, A.D. A new mixing of Hartree–Fock and local density-functional theories. *J. Chem. Phys.* **1993**, *98*, 1372–1377. [CrossRef]
35. Koch, W.; Holthausen, M.C. *A Chemist's Guide to Density Functional Theory*; John Wiley & Sons: Hoboken, NJ, USA, 2015. [CrossRef]
36. Domingo, L.R.; Ríos-Gutiérrez, M.; Pérez, P. Applications of the conceptual density functional theory indices to organic chemistry reactivity. *Molecules* **2016**, *21*, 748. [CrossRef]
37. Parr, R.G.; Yang, W. Density functional approach to the frontier-electron theory of chemical reactivity. *J. Am. Chem. Soc.* **1984**, *106*, 4049–4050. [CrossRef]
38. Parr, R.G.; Szentpály, L.V.; Liu, S. Electrophilicity index. *J. Am. Chem. Soc.* **1999**, *121*, 1922–1924. [CrossRef]
39. Okulik, N.; Jubert, A.H. Theoretical study on the structure and reactive sites of non-steroidal anti-inflammatory drugs. *J. Mol. Struct. Theochem* **2004**, *682*, 55–62. [CrossRef]

Disclaimer/Publisher's Note: The statements, opinions and data contained in all publications are solely those of the individual author(s) and contributor(s) and not of MDPI and/or the editor(s). MDPI and/or the editor(s) disclaim responsibility for any injury to people or property resulting from any ideas, methods, instructions or products referred to in the content.